J. theor. Biol. (1984) **111**, 755-785

Asymptotic Forms of Tracer Clearance Curves: Theory and Applications of Improved Extrapolations

LUDVIK BASS, JANET AISBETT AND ANTHONY J. BRACKEN

Department of Mathematics, University of Queensland, Brisbane, Australia

(*Received* 7 *December* 1983, *and in final form* 25 *June* 1984)

Tracer clearance curves are conventionally extrapolated beyond times of observation by using monoexponential asymptotic forms. The inadequacy of the resulting predictions, especially as to the mean transit time and quantities derived from it, has been previously demonstrated experimentally.

Here improvements in extrapolations and in the resulting predictions are derived theoretically and tested on previously published data, venous as well as externally recorded. First, secure lower bounds on the mean transit times are constructed, and shown to be much higher than conventional outright estimates for venous data (twice as high in some cases). Next, new asymptotic forms of tracer clearance curves from kinetically heterogeneous systems are derived; they are not monoexponential, but they are as robust, contain as few parameters and are as easily connected to data. It is shown theoretically that for real organs these new asymptotic forms should extrapolate and predict better than monoexponentials, and this is demonstrated on previously published venous data from perfused muscle. In particular, the resulting outright predictions of mean transit times are substantially better than the best lower bounds. Furthermore, a correction is derived to the standard estimate of the rate of regional cerebral blood flow. In an application to previously published data recorded externally, that correction reduces the estimated flow rate by 4%.

1. Introduction

Major physiological conclusions from tracer kinetic data depend on extrapolations of tracer clearance (disappearance) curves beyond the times of observations. This dependence is particularly pronounced for quantities (such as volumes of distribution of indicators, or regional blood flows: e.g., Lassen & Perl, 1979) determined by the mean transit time of the tracer through the domain of interest, because very long transit times can make an important contribution to the mean even when they are infrequent. Even more sensitive to extrapolation are quantities that depend on the mean

0022-5193/84/240755+31 $03.00/0

square transit time, such as the variance of transit times (Homer & Weathersby 1980, Bass 1982).

A standard monoexponential extrapolation of tracer clearance curves has been used routinely for a long time in experimental and clinical work (Lassen & Perl, 1979), especially to correct for effects of the recirculation of tracers which obscures the frequency function of transit times in intact subjects. In a fundamental study of the extrapolation problem, Lassen & Sejrsen (1971) reviewed the theoretical basis of the standard monoexponential extrapolation method, and subjected that method to the most rigorous and complete experimental testing that we could find in the literature. Accurate measurements of ^{51}Cr-EDTA and ^{131}I-thalamate tracer activities, both venous and external, in cat gastrocnemius muscle (once-through perfusion) were continued for two hours. After a sufficiently long time the experimental results were consistent with a monoexponential asymptotic form of tracer clearance curves, but "sufficiently long" turned out to be in excess of half an hour. For example, when the standard monoexponential extrapolation was applied to the venous outflow of ^{51}Cr-EDTA after 1 min as if no later data were available, the predicted recovery of the radioactive dose was 83·2% of the actual dose, but the predicted mean transit time was only 19% of the true (two-hour) value. The corresponding predictions made after 10 minutes were 98·5% and 59%, respectively (Lassen & Sejrsen 1971, experiment 5). Since extrapolations are commonly needed and used between 1 and 10 minutes, the ultimate experimental success of the standard monoexponential extrapolation comes too late for many practical applications.

These practical shortcomings of currently used extrapolations underline the need for improved extrapolation procedures which would be theoretically justified and more effective in practice. This challenge is increased by the requirement that any useful asymptotic form of the tracer clearance curve should be independent of the initial distribution of tracer (e.g., of the detailed shape of the input bolus); its mathematical form should be so simple as to be connected to the available data by the choice of a few parameters, preferably only two, as in the case of the monoexponential. We require moreover that the improved extrapolations should be no less robust (stable), with respect to experimental errors or premature fitting, than monoexponential extrapolations.

In the present paper we develop, and test on existing experimental data, two methods of improved extrapolation with special emphasis on improved predictions of mean transit times $\bar{t}$. In the first part of the paper (section 4) we use the monoexponential asymptotic form to construct secure lower bounds on $\bar{t}$ which are substantially higher than the standard venous estimate (which is thereby superseded). For example, the aforementioned predictions

of $\bar{t}$ are improved from 19% to at least 44% at 1 minute, and from 59% to at least 78% at 10 min, from the same venous data. Even better results are obtained for the mean transit time of ^{131}I-thalamate (Table 1). In Appendix A we prove that the highest of our lower bounds is, in an appropriate sense, the best possible lower bound on $\bar{t}$. Upper bounds on $\bar{t}$ are discussed in Appendix B.

In the second part of the paper (sections 5-7) we turn to outright estimates (in place of bounds) of $\bar{t}$, applicable to external as well as to venous recordings. We relate the practical deficiencies of the standard monoexponential extrapolation method to fundamental questions as to its theoretical basis: what is a compartment in kinetic analysis (Rescigno, Lambrecht & Duncan, 1983), and how many similar but non-identical compartments comprise a capillary bed? The latter of these physiological questions will be shown to have its mathematical counterpart in a question as to which of two non-commutative limiting processes is to be taken first. From such considerations we arrive at a new asymptotic form for clearance curves which is not monoexponential, but which is independent of initial conditions in the same sense as the monoexponential. We show that the new asymptotic form is either attained before the monoexponential form, or replaces it altogether (depending on the kinetic heterogeneity of the perfused domain).

The new asymptotic form predicts, for clearance curves from once-through perfused organs, that at late times the *logarithm* of tracer activity (venous or externally recorded) is a convex function of time. This is invariably observed (and we assume it in the first part of the paper), but it is deducible in terms of compartmental models only with the aid of certain physiologically based assumptions, which we specify in section 3.

We demonstrate from the venous data of Lassen & Sejrsen (1971) that extrapolations based on the new asymptotic form give better agreement with experiments, and in particular substantially better outright estimates of $\bar{t}$, than extrapolations based on the monoexponential. In an application to externally recorded data from a human brain (Lassen *et al.*, 1963), we reduce by some 4% the standard estimate of cerebral blood flow in the temporal region.

2. Tracer Clearance Curves at Long Times

For well-known steps leading to our point of departure, we refer to the detailed presentation by Lassen & Sejrsen (1971) and to references therein. Briefly, an organ is perfused by steady blood flow (at the rate F) which is manifolded through the many capillaries of the organ and reunites in the vein. After a bolus of (intravascular or diffusible) tracer has entered the

organ, the mixing of capillary outputs in the vein yields the successive venous samples having the observed activity $c_v(t)$ (dilution curve) which determines the normalized frequency function (probability density) $h(t)$ of transit times t: if the bolus contained the dose m_0, then

$$h(t) = Fc_v(t)/m_0. \tag{1}$$

This definition ensures normalization of $h(t)$, since all indicator must ultimately be carried out of the organ by the outflux Fc_v:

$$\int_0^\infty h \, dt = 1. \tag{2}$$

(If F has not been measured, approximate normalization is obtained by dividing $c_v(t)$ by the area under that curve, observed and extrapolated.) From now on we shall set $m_0 = 1$: the choice of a *unit dose* does not reduce the generality of the work.

The residue of the unit dose, $m(t)$, remaining in the organ at any time $t > 0$ (the part which is yet to appear in the vein) is

$$m(t) = \int_t^\infty Fc_v(\tau) \, d\tau = \int_t^\infty h(\tau) \, d\tau, \tag{3}$$

so that

$$-\dot{m} = h. \tag{4}$$

(Here and below, a dot denotes differentiation with respect to time.) It is the quantity $m(t)$ that is observed by external recording, independently of observations of $c_v(t)$. If the second time-derivative of h (or of m) is positive throughout some time-interval, we say that $h(t)$ (or $m(t)$) is a convex function on that time-interval. If the second time-derivative of $\ln h$ (or of $\ln m$) is positive, we say that $h(t)$ (or $m(t)$) is a *logarithmically* convex function. If the signs of the second derivatives are reversed, we speak of concavity and of logarithmic concavity.

The present work deals with asymptotic forms of $h(t)$ and $m(t)$ at long times. We are therefore not concerned with any brief initial rise and concavity of $h(t)$; we consider only times long enough for the convexity of $h(t)$ and $m(t)$ to have become established:

$$\ddot{m} > 0 \; (\dot{h} < 0), \qquad \ddot{h} > 0. \tag{5}$$

If the organ is modelled as a set of $N+1$ compartments (labelled $i = 0, 1, \ldots, N$) taking up, exchanging and releasing tracer, it is well known that the time-dependence of $h(t)$ is given by the sum over the organ of the

contributions from individual compartments, as follows:

$$h(t) = \sum_{i=0}^{N} \left(\sum_{k=0}^{N} C_{ik} \, \mathrm{e}^{-\alpha_k t} \right) = \sum_{k=0}^{N} G_k \, e^{-\alpha_k t} \tag{6}$$

with constants C_{ik}, G_k:

$$\sum_{i=0}^{N} C_{ik} = G_k, \qquad k = 0, 1, \ldots, N \tag{7}$$

and with a set (spectrum) $\{\alpha_k\}$ of positive exponential constants:

$$0 < \alpha_0 < \alpha_1 < \ldots \alpha_N. \tag{8}$$

We see from equations (3) and (6) that $m(t)$ has the same mathematical form as $h(t)$, with G_k/α_k in place of G_k in equation (6). Whereas the constants C_{ik} and G_k carry the influence of initial conditions, asymptotic forms of $h(t)$ and $m(t)$ useful at long times must be determined primarily by the nature of the spectrum $\{\alpha_k\}$. It is clear that as time increases, the smallest α_k's will become increasingly influential in equation (6). One may then form a picture of contributions from "bad sites" (releasing tracer slowly) dominating increasingly over contributions from "good sites". That picture elucidates the exponential terms in equations (6) directly in terms of Poisson processes of tracer release at long times but, inasmuch as the compartments exchange tracer even before the mixing of capillary outputs in the vein, the constants α_k are not uniquely associated with spatial sites in the organ (Lassen & Sejrsen, 1971). In this final clearance of tracer, with which the present paper is concerned, the compartmental model is at its best. By contrast, early parts of $h(t)$ and $m(t)$ depend strongly on the distribution of lengths of pathways of blood through the organ (convective spaghetti: Lassen & Perl, 1979) which does not fit naturally into a compartmental picture. To form an idea of "early" in this context, we note that in the experiments of Lassen & Sejrsen (1971) the true mean transit time of a tracer confined to the blood (T1824 albumin) was ten times shorter than the true mean transit times of the two diffusible tracers discussed below.

The limitation of the compartmental approach at early times is revealed in mathematical terms when modelling of tracer transport through an organ includes convection and diffusion explicitly. In the model of Perl & Chinard (1968) the clearance curve (deduced from a partial differential equation) is given at late times by a convergent series of exponentials, as in equation (6) with $N = \infty$; but the series diverges at early times.

At long times $h(t)$ and $m(t)$ will appear as monoexponential functions if and when the exponential term associated with the smallest exponential constant, α_0 in the spectrum (8), comes to dominate the sum in equation

(6). We shall consider this in detail in sections 5 and 6. Here we note only that, since h is always non-negative, this limit implies that the constant G_0 in equations (6) and (7) must be positive; this in turn ensures the validity of inequalities (5) at sufficiently long times. The late convexity of $h(t)$ and of $m(t)$ is therefore explained by the compartmental model.

Since $m(t)$ and $h(t)$ tend to monoexponentials at long times, it seems natural to extrapolate them by suitably chosen monoexponential functions. We conclude this Section by recalling the standard monoexponential extrapolations, and the associated estimates of mean transit times, for venous and for externally recorded data (Lassen & Perl, 1979). If $h(t)$ or $m(t)$ is known for all times t, the mean transit time is

$$\bar{t} = \int_0^\infty th \, dt = \int_0^\infty m \, dt, \tag{9}$$

where the second equality follows by using equation (4) and integrating by parts. However, data are available only up to some time t_0, beyond which h or m is extrapolated to estimate $\bar{t}$.

Venous observations of $h(t)$ up to some time t_0 are extrapolated to all $t > t_0$ by the monoexponential function $h^*(t)$ which joins $h(t)$ at $t = t_0$ with continuous h and $\dot{h}$ (and hence $\dot{h}/h$). Evidently,

$$h^*(t) = h(t_0)\, e^{-\eta(t-t_0)}, \qquad t > t_0 \tag{10}$$

where

$$\eta = -\frac{\dot{h}(t_0)}{h(t_0)} > 0 \tag{11}$$

is the magnitude of the logarithmic derivative (slope of the semilogarithmic plot of $\ln h$ against t) seen at $t = t_0$. We denote the resulting estimate of $\bar{t}$ by $\bar{t}^*$. From equations (9) and (10),

$$\bar{t}^* = \int_0^{t_0} th \, dt + \int_{t_0}^\infty th^* \, dt = \int_0^{t_0} th \, dt + h(t_0)\frac{\eta t_0 + 1}{\eta^2}. \tag{12}$$

Observations of $m(t)$ recorded externally up to the time t_0 are extrapolated to all $t > t_0$ by the monoexponential function $m^*(t)$ which joins $m(t)$ at $t = t_0$ with continuous m and $\dot{m}$;

$$m^*(t) = m(t_0)\, e^{-\mu(t-t_0)}, \qquad t > t_0, \tag{13}$$

where

$$\mu = -\frac{\dot{m}(t_0)}{m(t_0)} > 0, \tag{14}$$

in correspondence with equations (10) and (11). We denote the resulting estimate of $\bar{t}$ by $\bar{t}_2^*$. From the last expression in equation (9),

$$\bar{t}_2^* = \int_0^{t_0} m \, dt + m(t_0)/\mu. \tag{15}$$

3. Convexity and Logarithmic Convexity of Late Clearance Curves

Suppose that the residue $m(t)$ is a logarithmically convex function at all $t > t_0$ (so that the semilogarithmic plot of $m(t)$ is convex). Since $\ln m^*(t)$ given by equations (13) and (14) is a linear function of time, tangent at $t = t_0$ to the convex $\ln m(t)$, $\ln m^*(t)$ must be below $\ln m(t)$ and so

$$m^*(t) < m(t), \qquad t > t_0. \tag{16}$$

Therefore $\bar{t}_2^*$ given by equation (15) is below the true value of $\bar{t}$ given by equation (9):

$$\bar{t}_2^* < \bar{t}. \tag{17}$$

If $m(t)$ is logarithmically concave for $t > t_0$, then $\bar{t}_2^* > \bar{t}$. Similarly, $\bar{t}^*$ given by equation (12) underestimates (overestimates) $\bar{t}$ if $h(t)$ is logarithmically convex (concave).

Evidently it is not convexity (concavity) but *logarithmic* convexity (concavity) that is decisive in deducing bounds on $\bar{t}$ by extrapolations. However, only convexity, expressed by relations (5), is guaranteed at late times by the compartmental model. This raises the question as to why, in once-through perfusions of real organs, $h(t)$ and $m(t)$ invariably develop logarithmic convexity in the course of time, as exemplified in Figs. 3 and 4 below.

To examine this question we write explicitly

$$d^2 \ln h/dt^2 = (\ddot{h}h - \dot{h}^2)/h^2. \tag{18}$$

We observe that if h is concave ($\ddot{h} < 0$), then it is logarithmically concave; but if h is convex (as it must become in time), it may be logarithmically convex or logarithmically concave. This important remark holds similarly for $m(t)$. Substituting $h(t)$ from equation (6) in equation (18), we find after some manipulation

$$\ddot{h}h - \dot{h}^2 = \tfrac{1}{2} \sum_{i=0}^{N} \sum_{k=0}^{N} (\alpha_i - \alpha_k)^2 G_i G_k \, e^{-(\alpha_i + \alpha_k)t}. \tag{19}$$

This sum of all members of a symmetric array (with zeros on the diagonal) is equal to twice the sum of all members on one side of the diagonal. For a non-zero sum we need at least two compartments.

Suppose first that there are just two compartments; the sum in equation (19) is reduced to one term, the sign of which is the sign of G_0G_1. Since $G_0>0$ and G_1 are constants, $\ddot{h}h-\dot{h}^2$ is permanently positive if $G_1>0$, and negative if $G_1<0$. Compartmental analysis permits therefore $h(t)$ (and $m(t)$) to be logarithmically concave at the same (late) times as it is convex. If there are $N+1$ compartments and hence $N(N+1)/2$ independent terms in equation (19), then the first term will dominate after a sufficiently long time because $\alpha_0+\alpha_1$ is the smallest of all combinations $\alpha_i+\alpha_k$ formed from the spectrum (8). Since $G_0>0$, then $G_1>0$ again implies logarithmic convexity and $G_1<0$ implies logarithmic concavity, but now only at sufficiently late times.

A physiologically relevant compartmental model which generates logarithmic concavity is as follows. Suppose that the extravascular space belonging to a single perfused capillary of an organ is represented as two compartments, one belonging to the upstream half of the capillary and the other to the downstream half; and suppose that the compartments are connected only by the unidirectional flow of the perfusate. Let extraction of tracer be so high that almost every tracer molecule in the unit bolus is first taken up by the upstream compartment, then released into the perfusate, then taken up by the second compartment, and then released and swept into the vein. One calculates easily (Lassen & Perl, 1979).

$$h=\frac{\alpha_0\alpha_1}{\alpha_1-\alpha_0}(e^{-\alpha_0 t}-e^{-\alpha_1 t}), \tag{20}$$

$$m=\frac{\alpha_1 e^{-\alpha_0 t}-\alpha_0 e^{-\alpha_1 t}}{\alpha_1-\alpha_0}. \tag{21}$$

Comparing with equation (6) we find $G_0=-G_1=\alpha_0\alpha_1/(\alpha_1-\alpha_0)>0$, so that $G_0G_1<0$. Hence h and m are logarithmically concave functions at all times, in contrast to the observed long-time behaviour of h and m from real organs. (The logarithmic concavity can be seen directly by differentiating $\ln h$ and $\ln m$ twice.)

To build up a picture of the organ, consider a second model capillary, with exponential constants $0<\alpha_0'<\alpha_1'$ corresponding to the constants $0<\alpha_0<\alpha_1$ of the first capillary. From real organs, especially capillary beds, we take as postulates: capillaries are arranged essentially in parallel (with outputs mixed in the vein); they are similar but not identical. The parallelity postulate implies that the total residue of two unit boluses is $m+m'$ where m' is as m in equation (21), but with α_1', α_0' in place of α_1, α_0. The non-identity postulate implies that α_0, α_1, α_0', α_1' are distinct. The similarity postulate implies that α_0 is close to α_0', and α_1 to α_1'. Therefore, since α_0

is below α_1, so is α_0'. Since α_0' is below α_1', so is α_0. Hence each of α_0 and α_0' is below both α_1 and α_1'. Since $G_0 > 0$ and $G_0' > 0$, logarithmic convexity of $m + m'$ (and hence of $h + h'$) at late times is assured.

Adding many more capillaries in this way, and relabelling constants consistently with the ordering (8), we see that $G_i > 0$ will be correlated with low α_i, $G_i < 0$ with large α_i. If we plot G_i against α_i, the resulting points will cluster above the α-axis when α_i is small, and below it when α_i is large; the points will be distributed along a curve $G(\alpha)$ such as is drawn in Fig. 1 below. For an organ comprising many capillaries, this picture is unlikely to change qualitatively if we introduce smaller extractions in the basic two-compartment element above, and permit some transfer of tracer between capillaries. For the purposes of the present work we require only that the positivity of G_i's belonging to the smallest α_i's be preserved in the transition to a real organ. We conclude that while a *small* compartmental system is capable of permanent or at least asymptotic logarithmic concavity of h and m, a sufficiently large compartmental system satisfying the foregoing physiological postulates must result in the observed logarithmic convexity at late times.

We close this Section with two remarks on logarithmic convexity which are relevant to what follows. Let $\dot{m} = -\dot{h} > 0$, and consider the meaning of the relation

$$-\dot{m}/m < -\dot{h}/h, \tag{22}$$

which states that ln h falls with time more steeply than ln m. At $t = t_0$ relation (22) becomes, according to equations (11) and (14),

$$\mu < \eta. \tag{23}$$

Since $h = -\dot{m}$ and $\dot{h} = -\ddot{m}$ according to equation (4), inequality (22) is equivalent to $\ddot{m}m > m^2$, which means that $m(t)$ is logarithmically convex. The inequality in relation (22) is replaced by equality if (and only if) m and h are monoexponential.

Suppose that $h(t)$ is logarithmically convex for all $t > t_0$, and consider the extrapolation of h by equations (10) and (11). The area under the extrapolation is easily calculated to be $h(t_0)/\eta$, and this must be less than the true area, which is $m(t_0)$ according to equation (3): $h(t_0) < \eta m(t_0)$. Using equations (4) and (11), this inequality becomes equivalent to inequality (23), which asserts the logarithmic convexity of $m(t)$ at $t = t_0$. But this reasoning holds if we replace t_0 by any t_0' (say) such that $t_0' > t_0$. Hence, if $h(t)$ is logarithmically convex for all $t > t_0$, so is $m(t)$. One can show further that the converse of this result does not hold (because the definition of logarithmic convexity of m, stated in terms of h, involves $\ddot{h}$).

The assumption of logarithmic convexity of $m(t)$ for all $t > t_0$ is therefore weaker (more general) than the corresponding assumption for $h(t)$.

4. Lower Bounds on Mean Transit Times

On the basis of the considerations of section 3, and of empirical observations, we assume from now on the existence of a time t_0 such that $m(t)$ is a logarithmically convex function for all $t \geq t_0$. We consider extrapolations of $m(t)$ and $h(t)$ for $t \geq t_0$, given data for $t \leq t_0$. Under these conditions the inequalities (17) and (23) are valid. In practice $m(t)$ will be logarithmically convex for some time before t_0, as in Fig. 4 below.

We introduce another estimate of the mean transit time $\bar{t}$ based on a monoexponential. In equation (12) for $\bar{t}^*$, the integral of th involves the empirically known $h(t)$ from $t = 0$ to $t = t_0$, and for $t > t_0$, $h(t)$ is replaced with $h^* < h$. Here h^* was used more than actually necessary: if we write equation (9) in the form

$$\bar{t} = \int_0^\infty th \, dt = \int_0^{t_0} th \, dt + t_0 \int_{t_0}^\infty h \, dt + \int_{t_0}^\infty (t - t_0) h \, dt \tag{24}$$

we need to replace h with h^* from equation (10) only in the last term, since the middle term is known from data ($h(t)$ being normalized). We thus obtain the estimate $\bar{t}_1^*$:

$$\bar{t}_1^* = \int_0^{t_0} th \, dt + t_0 \left(1 - \int_0^{t_0} h \, dt \right) + h(t_0)/\eta^2, \tag{25}$$

expressed entirely in terms of h given at $t \leq t_0$.

We have three estimates of $\bar{t}$, given by equations (12), (15) and (25); we now compare them with $\bar{t}$ and with each other. From equations (25) and (12) we have

$$\bar{t}_1^* - \bar{t}^* = t_0 h(t_0) \left[\int_{t_0}^\infty h \, dt / h(t_0) - \eta^{-1} \right]. \tag{26}$$

From equations (3), (4) and (14) we see that the bracketed term in equation (26) is $\mu^{-1} - \eta^{-1}$; from inequality (23) we conclude that $\bar{t}_1^* > \bar{t}^*$.

Using equation (4) in integrating by parts the first term in equation (15), we find

$$\int_0^{t_0} m \, dt = \int_0^{t_0} th \, dt + t_0 \left(1 - \int_0^{t_0} h \, dt \right). \tag{27}$$

From equations (15), (25) and (27) we find

$$\bar{t}_2^* - \bar{t}_1^* = m(t_0)/\mu - h(t_0)/\eta^2 = h(t_0)(\mu^{-2} - \eta^{-2}), \tag{28}$$

where we used equations (4) and (14) to deduce the last equality. From inequality (23) we conclude that $\bar{t}_2^* > \bar{t}_1^*$. Using also inequality (17), we obtain the sequence of inequalities

$$\bar{t}^* < \bar{t}_1^* < \bar{t}_2^* < \bar{t}. \tag{29}$$

Thus $\bar{t}^*$, $\bar{t}_1^*$ and $\bar{t}_2^*$ are all lower bounds on $\bar{t}$. Since $\bar{t}_2^*$ is the best (highest) of them, it is important to transform it for use with venous data, such as we shall analyse below. Using equations (27), (14), (2), (3) and (4), we find that equation (15) can be rewritten:

$$\bar{t}_2^* = \int_0^{t_0} th \, dt + t_0\left(1 - \int_0^{t_0} h \, dt\right) + \left(1 - \int_0^{t_0} h \, dt\right)^2 \Big/ h(t_0) \tag{30}$$

which is expressed entirely in terms of venous data up to the time t_0.

Since $\bar{t}_2^*$ was obtained from a monoexponential extrapolation of $m(t)$ for $t > t_0$, equations (4) and (9) show that it must also be obtainable from a monoexponential extrapolation of $h(t)$ for $t > t_0$, say $\tilde{h}(t)$. How does $\tilde{h}(t)$ differ from $h^*(t)$ given by equations (10) and (11)? The continuity of $\dot{m}(t)$ and $m(t)$ at $t = t_0$ means, in terms of h, that $h(t_0)$ is continuous at t_0, and that the area under $\tilde{h}(t)$, $t > t_0$, is such as to preserve the normalization of the complete $h(t)$ (observed and extrapolated). This determines the two parameters available in a monoexponential; $\tilde{h}(t_0)$ cannot therefore be made equal to $\dot{h}(t_0)$. Thus extrapolation by $\tilde{h}(t)$, leading to $\bar{t}_2^*$, involves a discontinuity in $\dot{h}$ at $t = t_0$. By contrast, extrapolation by $h^*(t)$, leading to $\bar{t}^*$ and $\bar{t}_1^*$, is continuous in h and $\dot{h}$, but does not preserve normalization of h. In general, a two-parametric extrapolation function such as the monoexponential cannot have preassigned values of h and $\dot{h}$ at the starting time $t = t_0$, as well as an area under it preassigned so as to normalize the complete $h(t)$ (observed and extrapolated); that would require an extrapolation function with at least three parameters.

Given that $m(t)$ is logarithmically convex for $t \geq t_0$, and given at t_0 only the three quantities

$$h(t_0), \dot{h}(t_0), \int_{t_0}^{\infty} h \, dt = m(t_0)$$

that have been used in constructing $\bar{t}^*$, $\bar{t}_1^*$ and $\bar{t}_2^*$, it is natural to ask whether still better (higher) lower bounds on $\bar{t}$ can be constructed. We show in Appendix A that the answer is negative: $\bar{t}_2^*$ is the best (highest) possible lower bound in this sense.

Are there also useful *upper* bounds on $\bar{t}$? It seems clear that $\bar{t}$ can be arbitrarily large if the smallest exponential constant, α_0, is sufficiently small. In Appendix B we construct the lowest upper bound that can be given in

terms only of α_0 and of quantities observed up to the time t_0, and we show explicitly how it tends to infinity as α_0 tends to zero. We then use this upper bound to test the extent to which asymptotic forms, developed in the second part of the paper, are applied prematurely to data extrapolation.

We now apply these results to the data obtained by Lassen & Sejrsen (1971) by venous recordings of two tracers from cat gastrocnemius muscle. In these experiments, $h(t)$ and $m(t)$ become convex and logarithmically convex after less than 0·5 min. From regressions of experimental data up to several values of t_0, Lassen & Sejrsen computed and tabulated three quantities: η given by equation (11); $\bar{t}^*$ given by equation (12); and the ultimate recovery of the tracer, predicted by extrapolation by means of equations (10) and (11), expressed as the fraction R^* of the actual dose:

$$R^* = \int_0^{t_0} h\,dt + \int_{t_0}^{\infty} h^*\,dt = \int_0^{t_0} h\,dt + \frac{h(t_0)}{\eta}. \tag{31}$$

(Since $h(t)$ was logarithmically convex at $t > t_0$ for each t_0, we have $h^*(t) < h(t)$ for $t > t_0$, and so $R^* < 1$.)

Using equations (31) and (12), respectively, we recover at each t_0 the empirical quantities

$$\int_0^{t_0} h\,dt = R^* - h(t_0)/\eta, \tag{32}$$

$$\int_0^{t_0} th\,dt = \bar{t}^* - h(t_0)(\eta t_0 + 1)/\eta^2 \tag{33}$$

in terms of quantities given by Lassen & Sejrsen and listed in the first five lines of Table 1. Thus the numerical values of the new estimates $\bar{t}_1^*$, $\bar{t}_2^*$ are determined from the venous data of Lassen & Sejrsen (1971) by means of equations (25) and (30). We list the resulting $\bar{t}_1^*$ in the sixth, $\bar{t}_2^*$ in the seventh line of Table 1. The successive improvements in the estimate of $\bar{t}$ are seen to be systematic (in accord with the inequalities (29)) and substantial in all entries. For thalamate at 25 min, $\bar{t}_2^*$ is indistinguishable from $\bar{t}$.

5. Asymptotic Forms of Tracer Clearance Curves

In the first part of this work we viewed the standard estimate $\bar{t}^*$ of the mean transit time, given by equation (12), as a secure *lower bound* on the time $\bar{t}$. A more usual interpretation of $\bar{t}^*$ is to regard it as an *outright estimate* of $\bar{t}$ based on the circumstance that the monoexponential $h^*(t)$, given by equations (10) and (11) and used in the calculation of $\bar{t}^*$, is an asymptotic form of equation (6) at very long times (Lassen & Sejrsen, 1971). From

TABLE 1

Venous recordings from cat gastrocnemius muscle: estimates of mean transit times by extrapolations from times t_0

	t_0 (min)		
	1	10	25
$t_0/\bar{t}$	0·565 (0·813)	5·65 (8·13)	14·7 (20·3)
h min^{-1}	$1{\cdot}70\times10^{-1}$ ($7{\cdot}35\times10^{-2}$)	$2{\cdot}94\times10^{-3}$ ($1{\cdot}04\times10^{-3}$)	$4{\cdot}62\times10^{-4}$ ($2{\cdot}30\times10^{-4}$)
η min^{-1}	2·888 (2·475)	0·277 (0·266)	0·0660 (0·0693)
R^*	0·832 (0·913)	0·985 (0·985)	0·9976 (0·9951)
$\bar{t}^*/\bar{t}$	0·19 (0·25)	0·59 (0·50)	0·84 (0·73)
$\bar{t}_1^*/\bar{t}$	0·28 (0·32)	0·67 (0·62)	0·88 (0·83)
$\bar{t}_2^*/\bar{t}$	0·44 (0·46)	0·78 (0·89)	0·92 (1·03)
$\bar{t}_1/\bar{t}$	0·29 (0·32)	0·68 (0·63)	0·94 (0·86)
$\bar{t}_2/\bar{t}$	0·53 (0·55)	0·81 (1·11)	0·95 (1·15)

Numbers outside brackets pertain to experiment 5 with ^{51}Cr-EDTA; inside brackets to experiment 7 with ^{131}I-thalamate; h is the frequency function of transit times, and $\eta = |\dot{h}/h|$; R^* is the fractional recovery of the dose predicted by standard monoexponential extrapolation of h from the time t_0 onwards; $\bar{t}$ is the true mean transit time. $\bar{t}^*$ is the standard estimate of $\bar{t}$; $\bar{t}_1^*$ and $\bar{t}_2^*$ are new lower bounds on $\bar{t}$; $\bar{t}_1$ and $\bar{t}_2$ are new outright estimates of $\bar{t}$, derived in section 7. The first five lines (Lassen & Sejrsen 1971, and private communications) contain all the data used in the calculations of the last four lines.

now on we shall adopt a similar point of view and seek an improved asymptotic form of equation (6) which will lead to improved outright estimates.

How is the monoexponential asymptotic form of equation (6) attained? The ratio of any kth term to the first one varies with time as $\exp[-(\alpha_k - \alpha_0)t]$; for $k > 0$ this becomes arbitrarily small at a sufficiently long time. Since $\alpha_1 - \alpha_0$ is the smallest of all the differences $\alpha_k - \alpha_0$, $k > 0$ (cf. relations (8)), any *one* term with $k > 0$ becomes negligible as compared with the first term when

$$(\alpha_1 - \alpha_0)t \gg 1; \tag{34}$$

this familiar condition is *necessary* for the attainment of the monoexponential asymptotic form $G_0 \exp(-\alpha_0 t)$. We note that the condition (relation (34)) is independent of the number $N+1$ of exponential terms in the series.

However, the asymptotic representation of the sum in equation (6) by its first term requires that the *sum* of the other N terms be relatively small, and the magnitude of that remainder sum at any time does depend on the number N of its terms. A *sufficient* condition for the representation of the sum in equation (6) by its first term may therefore be expected to depend on N as well as on t. For fixed α_0 and for α_N bounded from above, such

a sufficient condition may then depend on the density of the spectrum (8) in such a way that the greater that density, the longer the time needed to satisfy the sufficient condition. It is for this reason that in the limit of a continuous spectrum we shall arrive at a new asymptotic form which is not monoexponential.

The derivation of equation (6) presupposes that the organ can be analysed into a finite number $(N+1)$ of distinct homogeneous compartments (Lassen & Sejrsen, 1971). However, the interplay of tracer uptake with unidirectional flow of perfusate generates spatial gradients of concentration which render any compartment of finite volume heterogeneous in the context of uptake (Bass *et al.* 1983). Thus the number of homogeneous compartments in a perfused organ is very large or, strictly speaking, infinite. Then the continuous spectrum

$$\alpha_0 \leq \alpha < \alpha_N \tag{35}$$

may be physiologically more appropriate than the discrete spectrum (8). We take account of this possibility by extending equation (6) to

$$h(t) = \int_{\alpha_0}^{\alpha_0+\Delta\alpha} G(\alpha)\, \mathrm{e}^{-\alpha t}\, \mathrm{d}\alpha, \tag{36}$$

where

$$\Delta\alpha = \alpha_N - \alpha_0 > 0 \tag{37}$$

may be infinite.

If there is a finite number $N+1$ of homogeneous compartments, or an infinite number of (infinitesimal) homogeneous compartments which nevertheless fall into a finite number $N+1$ of distinct classes, we recover equation (6) from equation (36) by setting

$$G(\alpha) = \sum_{k=0}^{N} G_k\, \delta(\alpha - \alpha_k), \tag{38}$$

where $\delta(\alpha - \alpha_k)$ are impulse (Dirac delta) functions. In this case the *kinetic heterogeneity* remains finite. If however the number of distinct classes is infinite (infinite kinetic heterogeneity), then $G(\alpha)$ in equation (36) may be a continuous function of α. In that case the asymptotic form of $h(t)$ at long times is not monoexponential, as we now show.

We assume that

$$\lim_{\alpha \to \alpha_0+} G(\alpha) = G(\alpha_0) > 0. \tag{39}$$

(For the case $G(\alpha_0) = 0$, see below.) We introduce the new integration variable

$$u = (\alpha - \alpha_0)t, \qquad \mathrm{d}u = t\, \mathrm{d}\alpha; \tag{40}$$

equation (36) becomes

$$h(t) = \frac{e^{-\alpha_0 t}}{t} \int_0^{t\Delta\alpha} G(\alpha_0 + u/t)\, e^{-u}\, du. \tag{41}$$

At long times, we have the precise result

$$\lim_{t\to\infty} (h(t)\, t\, e^{\alpha_0 t}) = G(\alpha_0) \int_0^{\infty} e^{-u}\, du = G(\alpha_0), \tag{42}$$

using equation (39). This means that, asymptotically

$$h(t) \approx G(\alpha_0)\, e^{-\alpha_0 t}/t. \tag{43}$$

For an intuitive appreciation of this key result, replace $G(\alpha)$ by the rectangular distribution $G(\alpha) = G(\alpha_0)$ between α_0 and $\alpha_0 + \Delta\alpha$, and $G(\alpha) = 0$ elsewhere. Then equation (36) yields by direct integration

$$h(t) = G(\alpha_0)(e^{-\alpha_0 t}/t)(1 - e^{-\Delta\alpha t}). \tag{44}$$

At large times, $\exp(-\Delta\alpha t) \ll 1$, the value of $\Delta\alpha$ becomes immaterial, and equation (43) approximates equation (44). That is: so long as $G(\alpha)$ is represented correctly near α_0, the effect of the errors $G(\alpha) - G(\alpha_0)$ at $\alpha > \alpha_0$ on the sum (integral) becomes relatively insignificant at times $t \gg 1/\Delta\alpha$. It is interesting and cautionary to note that as long as $t\Delta\alpha$ is small (as can happen even at long times for a sufficiently narrow spectrum (8)), equation (44) simulates a monoexponential, from which it deviates at later times. In the following applications of equation (43), α_0 and $G(\alpha_0)$ will be estimated from data, whereby equation (39) defines an empirical representation of the effective part of $G(\alpha)$. In practice equation (43) may be applied prematurely, so that the estimated value of α_0 may differ from the true one. In what follows we shall denote by γ the empirical estimate of α_0. When $h(t)$ is extrapolated continuously for $t \geq t_0$ by equation (43), we have

$$h = h(t_0)\, t_0\, e^{-\gamma(t-t_0)}/t, \qquad t \geq t_0, \tag{45}$$

where γ remains to be determined from data (see section 7). Equation (45) corresponds to equation (10) used in monoexponential extrapolations. The form of $G(\alpha)$ which would lead exactly to equation (45) through equation (36) with $\Delta\alpha = \infty$ is evidently

$$G(\alpha) = h(t_0)\, t_0\, e^{\gamma t_0} H(\alpha - \gamma) \tag{46}$$

where $H(x)$ is the step function equal to zero for $x < 0$ and to unity for $x \geq 0$. The form of $G(\alpha)$ which would lead exactly to equation (10) is, by contrast,

$$G(\alpha) = h(t_0)\, e^{\eta t_0} \delta(\alpha - \eta) \tag{47}$$

where δ is the impulse (Dirac) function. Thus the forms given by equations (45) or (10) may be viewed as consequences of approximating the true $G(\alpha)$ by equations (46) or (47), respectively. We represent these relations schematically in Fig. 1. We shall see below that as t_0 increases, η and γ approach α_0 while preserving the ordering $\alpha_0 < \gamma < \eta$.

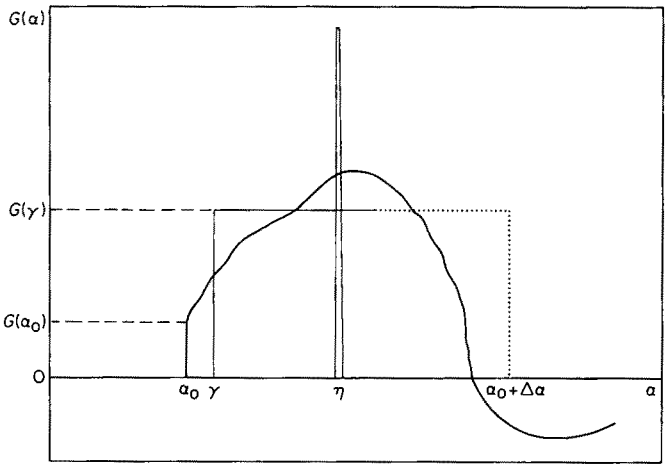

FIG. 1. A continuous spectrum of exponential constants α, with distributions of their weights $G(\alpha)$. The peaked distribution at $\alpha = \eta$ produces the familiar monoexponential asymptotic form of the tracer clearance curve, the step at $\alpha = \gamma$ the new asymptotic form. The rectangular distribution facilitates the discussion in the text.

Consideration of Fig. 1 suggests that equations (39) and (46) may yield effective representations of $G(\alpha)$, but even better representations may be obtained by allowing for the possibility that $G(\alpha_0) = 0$. In Appendix C we derive the asymptotic form of $h(t)$ for this case. This interesting form contains three parameters, so that its success in extrapolations would not be comparable with the successes of extrapolations by two-parametric asymptotic forms such as the monoexponential, and the new form given by equations (43) and (45). We shall therefore not apply the three-parametric form to data in the present paper.

Next we deduce the form of $m(t)$ by integrating $h(t)$ according to equation (3). If $h(t)$ has the general form given by equation (36), we find readily

$$m(t) = \int_{\alpha_0}^{\alpha_0+\Delta\alpha} \frac{G(\alpha)}{\alpha} e^{-\alpha t} \, d\alpha \tag{48}$$

which differs from $h(t)$ merely by having $G(\alpha)/\alpha$ in place of $G(\alpha)$. It is apparent from a comparison of equations (36) and (48) that $m(t)$ approaches

its asymptotic state faster than $h(t)$, because the division of $G(\alpha)$ by α in the integrand of equation (48) diminishes particularly those contributions to the integral which are to be relatively diminished in the course of time.

The foregoing steps leading to equation (43) now go through to the asymptotic form

$$m(t) \approx G(\alpha_0)\frac{e^{-\alpha_0 t}}{\alpha_0 t} \quad \text{as} \quad t \to \infty, \tag{49}$$

so that the limiting ratio $h(t)/m(t)$ tends to the constant α_0: at long times, $\ln m(t)$ and $\ln h(t)$ tend to become *parallel*. As in the case of finite kinetic heterogeneity leading to the limiting monoexponential, such parallelity between data recorded externally and from the vein signifies that the asymptotic state has been approached. However, while the monoexponential asymptotic form is characterized by rectilinear plots of $\ln h(t)$ and $\ln m(t)$, the corresponding plots of equations (43) and (49) are convex, tending to rectilinearity only when $\alpha_0 \gg 1/t$:

$$d \ln h/dt = d \ln m/dt = -\alpha_0 - \frac{1}{t}, \tag{50}$$

with second derivatives equal to $1/t^2$.

We test this important distinction in Fig. 2 on the data of Lassen & Sejrsen (1971, Fig. 1) relating to the longest transit times of ^{51}Cr-EDTA through

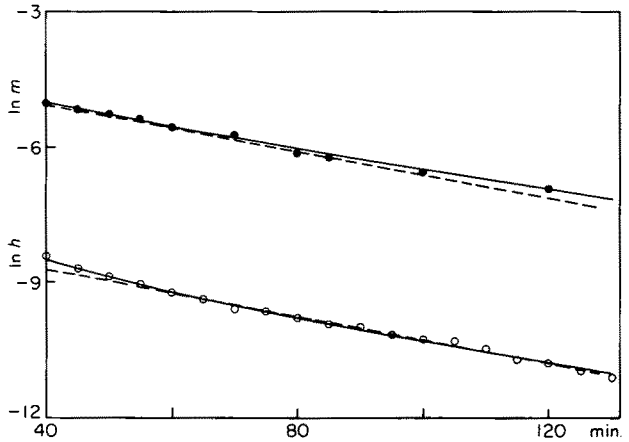

FIG. 2. Final clearance of ^{51}Cr-EDTA tracer from cat gastrocnemius muscle. Venous data (open circles) determining the frequency function $h(t)$ of transit times, and externally recorded data (closed circles) determining the fractional residue $m(t)$, are from Lassen & Sejrsen (1971, Fig. 1). A monoexponential (lower broken line) and the new asymptotic form (lower solid line) were fitted to the venous data between 55 min and 130 min. The corresponding upper lines, obtained from the lower ones by integration, predict the time-course of the residue.

cat muscle. The venous data (open circles, lower plot) were fitted between 55 and 130 min by a monoexponential, using linear regression of ln h against t; and by the regression of ln (th) against t, which is likewise linear according to equation (43). The models thus obtained are shown plotted over the range from 40 to 130 min as the lower broken curve and the lower solid curve, respectively. Both fit the data satisfactorily; the slight curvature of the solid line appears to improve the fit. When the two forms of $h(t)$ so fitted are integrated according to equation (3), the corresponding upper lines in Fig. 2 are obtained. Both are seen to fit equally well the externally recorded data (closed circles) from the same preparation (Lassen & Sejrsen 1971, Fig. 1). We note that when applied to extrapolations of the data from 130 min onwards, both forms of $h(t)$ yield practically identical values of the true mean transit time $\bar{t}$ (Table 1).

The satisfactory interpretation of the data in Fig. 2 in terms of the new asymptotic form demonstrates that, even when empirical plots of ln h and ln m at long times are consistent with rectilinearity and parallelity, one need not infer that a "final monoexponential" has been reached.

6. Interchange of Limiting Processes: an Illustrative Example

The appearance of two distinct asymptotic forms of clearance curves at long times (equations (10) and (43)) remains surprising until the connection between them is clarified more fully. The question whether the kinetic heterogeneity of a particular organ is infinite or merely very large seems rather theoretical, and one may ask instead which asymptotic form should be preferred for practical extrapolation if the spectrum (8) of α_k's is discrete but so dense that the sum in equation (6) could be approximated closely by the integral in equation (36) in the time-domain of interest.

In order to see the essentials we take equal differences between neighbouring α_k's throughout the width $\alpha_N - \alpha_0 = \Delta\alpha$ of the spectrum:

$$\alpha_1 - \alpha_0 = \alpha_2 - \alpha_1 = \ldots = \alpha_N - \alpha_{N-1} = \frac{\Delta\alpha}{N}, \tag{51}$$

and put all G_k in equation (6) equal to each other. Then equation (6) becomes

$$h(t) = \frac{h(0)}{N+1} e^{-\alpha_0 t} \sum_{k=0}^{N} e^{-k(\Delta\alpha/N)t}, \tag{52}$$

where the initial value $h(0)$ is the sum of the (equal) G_k's. The sum of this

geometric series is

$$h(t)=\frac{h(0)}{N+1}\,e^{-\alpha_0 t}\,\frac{1-e^{-(\Delta\alpha/N)(1+N)t}}{1-e^{-(\Delta\alpha/N)t}}. \tag{53}$$

If $t\to\infty$ at some fixed N (no matter how large), we approach the monoexponential limit

$$h(t)=h(0)\,e^{-\alpha_0 t}/(N+1). \tag{54}$$

If we *then* take N arbitrarily large (at fixed $\Delta\alpha$), the form of $h(t)$ in equation (54) remains monoexponential. By contrast, if we first proceed to the limit $N\to\infty$ (with fixed $\Delta\alpha$) at some finite time, no matter how large, we can expand the exponential in the denominator of equation (53) and obtain:

$$h(t)=\frac{h(0)}{\Delta\alpha}\;\frac{e^{-\alpha_0 t}}{t}(1-e^{-\Delta\alpha t}) \tag{55}$$

which has the same form as equation (44). If we then proceed to the limit of large t, we arrive at the asymptotic form given by equation (43), with $\Delta\alpha G(\alpha_0)=h(0)$. The limiting processes $N\to\infty$, $t\to\infty$ are *not commutative*; if they are interchanged, the two asymptotic forms are interchanged.

We can now return to the foregoing question concerning the long-time effects of a dense but discrete spectrum (8). The long-time behaviour of equation (53) falls into two successive regimes. The earlier regime is characterized by the inequalities

$$N\gg\Delta\alpha\,.\,t\gg 1, \tag{56}$$

which reduce equation (53) to equation (43). The other regime is reached much later still, when

$$N\ll\Delta\alpha\,.\,t, \tag{57}$$

whereby equation (53) yields the monoexponential form in equation (54). The influence of the width $\Delta\alpha$ of the spectrum on these considerations is apparent from the foregoing equations.

Because the limiting processes $t\to\infty$ and $N\to\infty$ are not commutative, the transition to the monoexponential cannot be made by increasing the variable t in equation (55): one must return first to equation (53). Despite this interesting mathematical detour, the monoexponential asymptotic form should be regarded as the ultimate limiting form of equation (55) when N is finite. However, when N is very large, the monoexponential form resulting from the attainment of equation (54) might never be seen experimentally because tracer activities could be too small to be detectable at the requisite

times. In that case our new asymptotic form (43) is the relevant one, even though N is finite.

We emphasize that the foregoing special choices of the sets α_k and G_k are made in this Section alone, in order to sum the series in equation (6) and hence to elucidate explicitly the relation between the two non-commutative limiting processes. The two resulting asymptotic forms are, of course, the same as those arrived at previously under more general assumptions.

7. Transit Times through Muscle and Brain: Outright Estimates of the Mean

We now apply the new asymptotic form to extrapolations of venous and of externally recorded clearance curves, and use them for outright estimates of the mean transit time $\bar{t}$.

We start again from equation (24), but in the last integral we now insert the new asymptotic form given by equation (45), which ensures continuity of h at $t = t_0$. (A simpler but poorer estimate of $\bar{t}$ would be obtained by proceeding similarly from equation (12).) We thus obtain

$$\bar{t} \approx \int_0^{t_0} th \, dt + t_0 \int_{t_0}^{\infty} h \, dt + \frac{t_0 h(t_0)}{\gamma} [1 - \gamma t_0 \, e^{\gamma t_0} E_1(\gamma t_0)], \tag{58}$$

where E_1 is the exponential integral

$$E_1(x) = \int_1^{\infty} \frac{e^{-xy}}{y} dy \tag{59}$$

tabulated in Abramowitz & Stegun (1965).

In determining the parameter γ from data there are alternatives which are analogous to those exploited in section 4 for extrapolations by mono-exponentials. Firstly, we can determine γ by making $\dot{h}$ (as well as h) continuous at $t = t_0$. Applying equation (50) at $t = t_0$ and using equation (11), we obtain

$$\gamma = \eta - 1/t_0. \tag{60}$$

We denote the estimate of $\bar{t}$ from equations (58) and (60) by $\bar{t}_1$. All the experimental results needed for the computation of $\bar{t}_1$ are contained in the first five lines of Table 1 (cf. equations (32) and (33)); the resulting values of $\bar{t}_1$ are listed in the penultimate line. As expected, $\bar{t}_1$ is much better throughout than the standard estimate $\bar{t}^*$. It is better than the lower bound $\bar{t}_1^*$, but substantially so only at $t_0 = 25$ min. However, $\bar{t}_1$ is below the best lower bound $\bar{t}_2^*$ in all cases except for EDTA at $t_0 = 25$ min.

Secondly, we can determine γ so that the area under $h(t)$ observed up to $t = t_0$, and the area under the extrapolation, add up to unity. Using equation (45) for the extrapolation, we obtain readily

$$\int_0^{t_0} h \, dt + t_0 h(t_0) \, e^{\gamma t_0} E_1(\gamma t_0) = 1. \tag{61}$$

We denote the estimate of $\bar{t}$ from equations (58) and (61) by $\bar{t}_2$. Using equation (61) to simplify equation (58), we obtain

$$\bar{t}_2 = \int_0^{t_0} th \, dt + t_0 h(t_0)/\gamma, \tag{62}$$

in which γ is still determined by equation (61). All the experimental results needed for the computation of $\bar{t}_2$ are again contained in the first five lines of Table 1. Using tables of E_1, we can readily estimate γt_0 (and hence γ) from equation (61): see Table 2 in Appendix B. The resulting values of $\bar{t}_2$ are listed in the last line of Table 1. The relative success of this estimate is evident by comparison with the preceding four lines, and is particularly important in practice at (or near) $t_0 = 1$ min. We note that a slight overestimate for thalamate at $t_0 = 10$ and 25 min persists unambiguously even when typical experimental errors are taken into consideration.

We turn to the practical problem of stability (robustness) of extrapolations with respect to experimental errors and premature applications of asymptotic forms (cf. Appendix B). The use of equation (60), leading to the estimate $\bar{t}_1$ of $\bar{t}$, is prone to generating instabilities, as follows. In general, a local determination of η (near some t_0) makes extrapolations sensitive to a small segment of the time-course of $h(t)$ or $m(t)$. In particular, if in that segment η happened to be equal to or less than $1/t_0$, the value of γ estimated from equation (60) would be zero or negative, and the resulting estimate $\bar{t}_1$ would be infinite. (By contrast, the estimate of $\bar{t}$ from any monoexponential extrapolation is finite so long as η is positive.) If we choose to extrapolate $m(t)$ by the asymptotic form given by equation (49), continuity of m and $\dot{m}$ at $t = t_0$ yields, in correspondence with equations (45) and (60) and using equation (14),

$$m = m(t_0) t_0 \, e^{-\gamma(t - t_0)}/t, \qquad t \geq t_0 \tag{63}$$

$$\gamma = \mu - 1/t_0, \tag{64}$$

from which another estimate of $\bar{t}$ is obtained by integrating $m(t)$ (observed and extrapolated) over all time (cf. equation (9)). However, because $\mu < \eta$ (inequality (23)), the instability associated with the possibility of estimating a negative γ at some t_0 is even greater when using equation (64) than when

using equation (60). We therefore do not use equations (63) and (64) any further.

The determination of $\bar{t}_2$ is, by contrast, as robust as estimates of $\bar{t}$ by monoexponential extrapolations. The value of γ is determined from equation (61) by finding γt_0 which satisfies

$$e^{\gamma t_0} E_1(\gamma t_0) = \left(1 - \int_0^{t_0} h \, dt\right) \Big/ t_0 h(t_0). \tag{65}$$

The positive quantity on the right-hand side is given experimentally at each t_0. Because the function $e^x E_1(x)$ falls monotonically from $+\infty$ at $x=0$ to 0 at $x = \infty$, a unique and positive γt_0 (and hence a finite $\bar{t}_2$) is always estimated from data. [From equation (59) we have

$$e^x E_1(x) = \int_1^\infty \frac{e^{-x(y-1)}}{y} \, dy,$$

which has evidently the value 0 at $x = \infty$, and $\ln(\infty) = \infty$ at $x=0$. Moreover,

$$\frac{d}{dx}(e^x E_1) = -\int_1^\infty \frac{y-1}{y} e^{-x(y-1)} \, dy < 0,$$

so that only one value of $x = \gamma t_0$ is found.] We conclude that equations (61) and (62) yield a combination of robustness and predictive power (see Table 1) which marks them as the best use of the new asymptotic form.

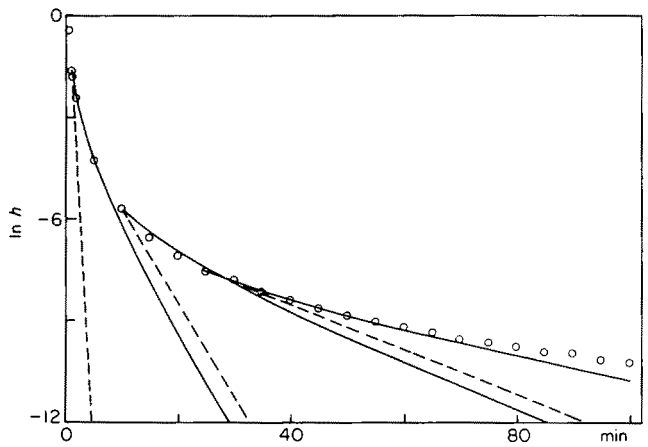

FIG. 3. Semilogarithmic plots of the frequency function $h(t)$ of transit times of ^{51}Cr-EDTA through cat gastrocnemius muscle. Venous data (open circles) of Lassen & Sejrsen (1971) are extrapolated from 1, 10 and 25 minutes onwards, using the monoexponential (broken lines) and the new asymptotic form (solid curves).

To examine this conclusion further, we show how equation (45) predicts the time-course of $h(t)$ for $t > t_0$ when γ is estimated from equation (61). Figure 3 shows venous data (open circles) of Lassen & Sejrsen (1971). In three separate pairs of regressions, the data were truncated to end at $t_0 = 1$, 10 and 25 min and then extrapolated using equations (45) and (61) (solid lines) and, for comparison, using equations (10) and (11) of the standard monoexponential extrapolation (broken lines). The superiority of the former over the latter extrapolation is apparent in all corresponding pairs, and it is reflected in the superiority of the estimate $\bar{t}_2$ over $\bar{t}^*$ in Table 1. However, all the extrapolations fall short of the data (the more so, the earlier they are made); this is because, as is usual in practice, the asymptotic forms are used before they are sufficiently closely attained (see also Appendix B).

An outstanding feature of the data of Lassen & Sejrsen (1971) is the provision of simultaneous venous and external recordings. This enables us to compare the residue $m(t)$, calculated by means of equation (3), with independent external measurements. In Fig. 4 the measurements (closed circles) are compared with predictions (solid and broken lines) obtained by integration from corresponding extrapolations of venous data in Fig. 3. The greater success of the new asymptotic form is again apparent in each pair of corresponding predictions. All predicted residues are too low because all extrapolated $h(t)$ in Fig. 3 are too low. There is a characteristic difference between the results of the two types of prediction. The residues predicted

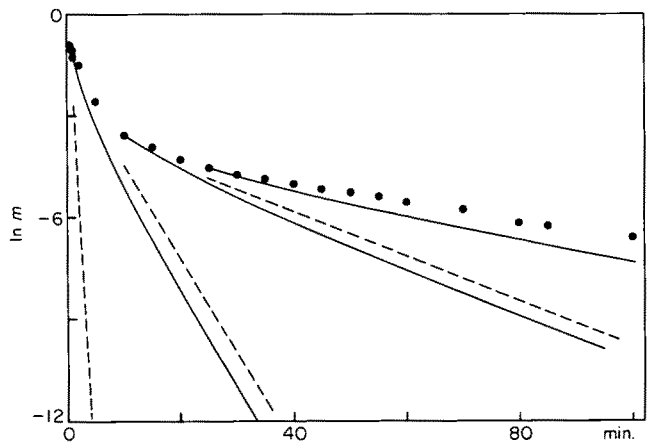

FIG. 4. Semilogarithmic time-courses of the fractional residue $m(t)$, predicted by integrating the extrapolations of $h(t)$ described in Fig. 3. The broken and solid lines are obtained by integrating the monoexponential and the new extrapolations, respectively. The predictions are to be compared with data (closed circles) recorded externally by Lassen & Sejrsen (1971).

from the standard monoexponential extrapolation (broken lines) are below the observed ones even at the times when $h(t)$ was fitted to data, because that extrapolation underestimates the area under the extrapolated venous curve. By contrast, the normalization-preserving predictions fit the data where $h(t)$ was fitted to the data (solid lines).

Equations (61) and (62) (or equivalently, (62) and (65)) are readily rewritten for use with externally recorded data. Using equations (2), (3) and (14), we see that the right-hand side of equation (65) is $(t_0\mu)^{-1}$, so that equation (65) becomes

$$\mu t_0 \, e^{\gamma t_0} E_1(\gamma t_0) = 1. \tag{66}$$

Next, we use equations (27), (2), (3) and the identity $h(t_0) = \mu m(t_0)$ (cf. equations (4) and (14)) to rewrite equation (62):

$$\bar{t}_2 = \int_0^{t_0} m \, dt + t_0 m(t_0)\left(\frac{\mu}{\gamma} - 1\right). \tag{67}$$

Another way of arriving at equations (66) and (67) is to form $m(t)$, $t > t_0$, by using equation (45) in equation (3); and then use it to extrapolate $m(t)$ with m and $\dot{m}$ continuous at $t = t_0$.

For the important class of experiments in which only externally recorded data are obtained, the standard estimate of $\bar{t}$ is $\bar{t}_2^*$ given by equation (15) (Lassen & Perl, 1979). For logarithmically convex $m(t)$, we have shown $\bar{t}_2^*$ to be an underestimate of $\bar{t}$. It differs from our best outright estimate, given by equation (67), by

$$\bar{t}_2 - \bar{t}_2^* = m(t_0)\left[t_0 \frac{\mu - \gamma}{\gamma} - \frac{1}{\mu}\right] \tag{68}$$

where γ is given by equation (66).

An important application of externally determined mean transit times is to regional cerebral blood flows, especially using inert gas tracers (Lassen & Perl, 1979). The rate f of the blood flow perfusing one gram of tissue in a region from which radioactivity is monitored externally, is

$$f = \lambda / \bar{t} \text{ ml} \cdot \text{g}^{-1} \cdot \text{min}^{-1}, \tag{69}$$

where λ is the empirically known tissue-blood partition coefficient. Since $\bar{t}_2^*$ is an underestimate of the true $\bar{t}$, its use in equation (69) yields an overestimate of f. The use of $\bar{t}_2$ in equation (69) yields a lower estimate of f. We consider the effect of the difference given by equation (68) on the estimated value of f. We denote the estimate $\lambda / \bar{t}_2^*$ by f_1, $\lambda / \bar{t}_2$ by f_2, and write

$$\frac{1}{f_2} - \frac{1}{f_1} = -\frac{f_2 - f_1}{f_1 f_2} = (\bar{t}_2 - \bar{t}_2^*)/\lambda. \tag{70}$$

When the magnitude of the (negative) change of $\delta f = f_2 - f_1$ in the estimate is small as compared with the true value of the flow, we can regard the geometric mean $(f_1 f_2)^{1/2}$ as being sufficiently close to the true f to be used in calculating the *relative* change $\delta f/f$ of the estimate of f:

$$\frac{\delta f}{f} \approx -\frac{f}{\lambda}(\bar{t}_2 - \bar{t}_2^*). \tag{71}$$

To illustrate the relevance of the foregoing considerations to clinical data (which are inevitably less precise and less extensive than data from animal experiments), we consider external recordings from the temporal area of the brain of patient No. 9 of Lassen *et al.* (1963, Fig. 2). These yielded $f \simeq 0{\cdot}64$ ml . g^{-1} . min^{-1}, and $\mu \simeq 0{\cdot}198$ min^{-1} from a linear regression of ln m against time for the late data. (For the ^{85}Kr tracer used, $\lambda \simeq 1$ ml . g^{-1}.) If we assume that the slope of the semi-logarithmic plot pertains to the mid-point of the linear regression ($t_0 \simeq 6$ min), we find $m(t_0) = 0{\cdot}0555$, and $\gamma = 0{\cdot}0975$ min^{-1} from equation (66). From equations (71) and (68) we then find $\delta f/f \simeq -0{\cdot}04$, that is, a reduction of 4% in the expectation value. This should be considered in relation to the experimental error of 6% (Lassen *et al.*, 1963).

The relative smallness of this correction illustrates the general observation of Lassen & Sejrsen (1971) that $\bar{t}$ is estimated better from externally recorded data than from venous data. The foregoing analysis shows more specifically that this is because the standard estimate $\bar{t}_2^*$ of $\bar{t}$ from externally recorded data corresponds, in terms of *venous* data, to the best lower bound on $\bar{t}$ rather than to the much lower standard estimate $\bar{t}^*$ (see Table 1).

We are grateful to Dr N. A. Lassen and Dr P. Sejrsen for additional information on their experiments; to them and to two referees for valuable comments; and to the Australian Research Grants Committee for financial support.

REFERENCES

ABRAMOWITZ, M. & STEGUN, I. A. (1965). *Handbook of Mathematical Functions.* New York: Dover Publications.

BASS, L. (1982). *J. theor. Biol.* **95**, 81.

BASS, L., BRACKEN, A. J. & BURDEN, C. J. (1983). *Tracer Kinetics and Physiologic Modeling* (Lambrecht, R. M. & Rescigno, A., eds), pp. 120–201. Lecture Notes in Biomathematics, Vol. 48. Berlin, Heidelberg, New York: Springer.

DOETSCH, G. (1974). *Introduction to the Theory and Application of the Laplace Transformation.* Berlin, Heidelberg, New York: Springer.

HOMER, L. D. & WEATHERSBY, P. K. (1980). *J. theor. Biol.* **87**, 349.

LASSEN, N. A., HØEDT-RASMUSSEN, K., SØRENSEN, S. C., SKINHØJ, E., CRONQUIST, S., BODFORSS, B. & INGVAR, D. H. (1963). *Neurology* **13**, 719.

LASSEN, N. A. & SEJRSEN, P. (1971). *Circ. Res.* **29**, 76.

LASSEN, N. A. & PERL, W. (1979). *Tracer Kinetic Methods in Medical Physiology.* New York: Raven Press.
PERL, W. & CHINARD, F. P. (1968). *Circ. Res.* **22,** 273.
RESCIGNO, A., LAMBRECHT, R. M. & DUNCAN, C. C. (1983). *Tracer Kinetics and Physiologic Modeling* (Lambrecht, R. M. & Rescigno, A., eds), pp. 59–119. Lecture Notes in Biomathematics, Vol. 48. Berlin, Heidelberg, New York: Springer.
TURNER, M. E. (1963). *Biometrics* **19,** 183.

APPENDIX A

Best Lower Bound on Mean Transit Time Determined from Venous Data

Suppose that venous data available at times $t \leq t_0$ determine the three fixed positive numbers A, V, D:

$$1 - \int_0^{t_0} h \, dt = \int_{t_0}^{\infty} h \, dt = A \tag{A1}$$

$$h(t_0) = V \tag{A2}$$

$$-\dot{h}(t_0) = D. \tag{A3}$$

In order to estimate the mean transit time (see equation (24)),

$$\bar{t} = \int_0^{t_0} th \, dt + t_0 A + Q \tag{A4}$$

where

$$Q = \int_{t_0}^{\infty} (t - t_0) h \, dt, \tag{A5}$$

we need to estimate Q by extrapolation of $h(t)$ to $t > t_0$. We assume that the true $h(t)$ and $\dot{h}(t)$ are continuous and, on the basis of the considerations of Section 3, that $\int_t^{\infty} h \, dt$ is a logarithmically convex function for $t \geq t_0$. This excludes monoexponentials from our considerations and in particular implies that at $t = t_0$

$$AD > V^2 \tag{A6}$$

which is equivalent to inequality (23). Then the sequence of inequalities (29) holds; the highest of these three lower bounds on $\bar{t}$ is $\bar{t}_2^*$, defined by

$$Q = A^2 / V \tag{A7}$$

according to equations (30) and (A4).

We now show that amongst all estimates of Q constructed in terms only of A, V and D, equation (A7) gives the highest lower bound on Q, so that

$\bar{t}_2^*$ is the best (highest) lower bound on $\bar{t}$. We prove this by constructing an $h(t)$ which is possibly true for times $t \geq t_0$ and yields a value of Q exceeding A^2/V by an arbitrarily small number. As the possibly true $h(t)$ at $t \geq t_0$ we choose

$$h(t) = C_0 e^{-\alpha_0(t-t_0)} + C_1 e^{-\alpha_1(t-t_0)}, \qquad t \geq t_0 \tag{A8}$$

with positive constants C_0, C_1, α_0, α_1. It is not difficult to check the following results. If we set

$$\alpha_0 = \frac{V}{A} - \varepsilon \tag{A9}$$

with *any* $\varepsilon > 0$ such that $\alpha_0 > 0$, then equations (A1), (A2) and (A3) are satisfied by equation (A8) with

$$\alpha_1 = \frac{AD - V^2 + \varepsilon AV}{\varepsilon A^2}, \tag{A10}$$

$$C_0 = \frac{(V - \varepsilon A)(AD - V^2)}{AD - V^2 + \varepsilon^2 A^2}, \tag{A11}$$

$$C_1 = \frac{\varepsilon A(AD - V^2 + \varepsilon AV)}{AD - V^2 + \varepsilon^2 A^2}. \tag{A12}$$

Moreover, the resulting value of Q is

$$Q = \frac{A^2}{V - \varepsilon A}\left[\frac{(AD - V^2)(AD - V^2 + \varepsilon AV) + \varepsilon^3 A^3 (V - \varepsilon A)}{(AD - V^2 + \varepsilon AV)(AD - V^2 + \varepsilon^2 A^2)}\right]. \tag{A13}$$

We are still free to choose ε in the interval $0 < \varepsilon < V/A$. We choose ε arbitrarily close to zero. Then, according to equation (A13), Q approximates A^2/V arbitrarily closely from above, as we set out to prove.

In this limiting process, C_0 tends to V and α_0 tends to V/A, while C_1 tends to zero as εA and α_1 tends to infinity as $(AD - V^2)/\varepsilon A^2$. We note that, although equation (A8) thus approaches a monoexponential for $t > t_0$, the contribution of the second exponential to $\dot{h}$ at $t = t_0$ (that is, $\alpha_1 C_1$) tends to the finite limit $D - V^2/A$. It is for this reason that equation (A3) and inequality (A6) remain satisfied in the limit. If we use equations (A8)-(A12) to construct $\bar{t}^*$ and $\bar{t}_1^*$ given by equations (11), (12) and (25), and proceed to the limit of vanishing ε, $\bar{t}^*$ and $\bar{t}_1^*$ remain below $\bar{t}_2^*$ because of their dependence on $\dot{h}(t_0)$.

If the foregoing assumption of logarithmic convexity was replaced by that of logarithmic concavity (and inequality (A6) was accordingly reversed), an analogous argument would show $\bar{t}_2^*$ to be the lowest (best)

upper bound on $\bar{t}$. Because of the considerations of section 3, this mathematical result seems to be physiologically uninteresting.

Higher moments of $h(t)$, such as the mean square transit time $\overline{t^2}$, can be estimated and bounded similarly. It is to be expected that the higher the moments, the more sensitive they are to extrapolations. We hope to return to these problems in a later paper.

APPENDIX B

Upper Bound on Mean Transit Times

We consider the mean transit time $\bar{t}$ in the form (see equation (9))

$$\bar{t} = \int_0^{t_0} m \, dt + \int_{t_0}^{\infty} m \, dt \tag{B1}$$

in which the second term is estimated by extrapolating $m(t)$ to $t > t_0$. We assume again that the true $m(t)$ is continuous, has a continuous derivative, and is a logarithmically convex function for $t \geq t_0$ (section 3).

Consider extrapolation by the function

$$m^{**} = m(t_0)\, e^{-\alpha_0 (t - t_0)}, \qquad t > t_0, \tag{B2}$$

where α_0 is the magnitude of the final slope of the semilogarithmic plot of $m(t)$; in terms of the spectrum (8), α_0 is its smallest element. At $t = t_0$ the extrapolation $m^{**}(t)$ joins $m(t)$ continuously, but with an upward jump in the slope. The linear function $\ln m^{**}(t)$ and the convex function $\ln m(t)$ coincide in their values at $t = t_0$, and in their slopes at $t = \infty$. Therefore $\ln m^{**} > \ln m$ for $t > t_0$, and

$$m^{**}(t) > m(t), \qquad t > t_0. \tag{B3}$$

It follows from equation (B1) that

$$\bar{t} < \int_0^{t_0} m \, dt + \int_{t_0}^{\infty} m^{**} \, dt = \bar{t}^{**}, \tag{B4}$$

defining an upper bound $\bar{t}^{**}$ on $\bar{t}$. From equations (B4) and (B2),

$$\bar{t}^{**} = \int_0^{t_0} m \, dt + m(t_0)/\alpha_0. \tag{B5}$$

To express $\bar{t}^{**}$ in terms of venous data, we use equations (2), (3), (27) and (B5):

$$\bar{t}^{**} = \int_0^{t_0} th \, dt + \left(1 - \int_0^{t_0} h \, dt\right)(t_0 + 1/\alpha_0), \tag{B6}$$

where all terms except α_0 are known from data at $t \leqslant t_0$. The equality $\bar{t} = \bar{t}^{**}$ would hold only if $h(t)$ was actually the monoexponential with the exponential constant α_0. Clearly there are many forms of $h(t)$ for which $\bar{t}^{**}$ is arbitrarily close to $\bar{t}$.

Unfortunately, the upper bound $\bar{t}^{**}$ is useless in the sense that by the time we can determine α_0 from data, no bound is needed because the monoexponential asymptotic form has been attained; and until we can determine α_0, it remains possible that α_0 will be arbitrarily small, rendering $\bar{t}^{**}$ arbitrarily large. It is clear that this feature of $\bar{t}^{**}$ must be shared by any upper bound on $\bar{t}$. Practical *predictive* work with bounds on $\bar{t}$ is therefore confined to lower bounds.

However, the two-hour data of Lassen & Sejrsen being available, $\bar{t}^{**}$ can be used for an additional *a posteriori* critique of the use of asymptotic forms at and after the times t_0 in Table 1. The standard monoexponential extrapolation approximates α_0 by η from equation (11), the extrapolation by the new asymptotic form approximates α_0 by γ from equation (61): see Fig. 1. We can therefore test the legitimacy of these extrapolations by inserting η and γ in place of α_0 in equation (B6), and demanding that the resulting approximation to $\bar{t}^{**}$, called $\bar{t}^{**}(\eta)$ and $\bar{t}^{**}(\gamma)$, respectively, should ideally be larger than the true $\bar{t}$. The results, normalized to the true $\bar{t}$, are collected in Table 2 in correspondence with Table 1. The relevant values of γ (solutions of equation (61)) are also listed.

Table 2 shows that all values of $\bar{t}^{**}(\gamma)/\bar{t}$ are above 0·75, and three are above unity. By contrast, all values of $\bar{t}^{**}(\eta)/\bar{t}$ are below unity, and four are below 0·75. This quantifies further the foregoing comments on Figs 3 and 4: the use of the new asymptotic form for extrapolation is shown to be premature in half the cases in Table 1, but much less so than the use of the standard monoexponential extrapolation.

TABLE 2

Approximate upper bounds on mean transit times

	t_0 (min)		
	1	10	25
γ (min^{-1})	0·25 (0·18)	0·054 (0·012)	0·024 (0·0088)
$\bar{t}^{**}(\eta)/\bar{t}$	0·31 (0·28)	0·70 (0·67)	0·90 (0·89)
$\bar{t}^{**}(\gamma)\bar{t}$	0·78 (0·84)	0·91 (1·77)	1·04 (1·55)

Approximations to an upper bound on the mean transit time $\bar{t}$ (normalized to the time $\bar{t}$), set out as in Table 1. Estimation of the smallest exponential constant α_0 by η (from Table 1) generates the second line; by γ (from first line) generates the third line.

APPENDIX C

A Three-parametric Asymptotic Form of Tracer Clearance

We begin again from equation (36) with an integrable $G(\alpha)$ in the interval $\alpha_0, \alpha_0+\Delta\alpha$ (with possibly infinite $\Delta\alpha$), and $G(\alpha)=0$ elsewhere. We consider the class of functions

$$G(\alpha)=(\alpha-\alpha_0)^\lambda F(\alpha) \tag{C1}$$

where $F(\alpha_0)>0$, and $\lambda>-1$ is a constant which determines how $G(\alpha)$ behaves as α tends to α_0 from the right. Using equation (C1) in equation (36), $h(t)$ becomes

$$h(t)=\int_{\alpha_0}^{\alpha_0+\Delta\alpha}(\alpha-\alpha_0)^\lambda F(\alpha)\,\mathrm{e}^{-\alpha t}\,\mathrm{d}\alpha. \tag{C2}$$

Using again the substitution $u=(\alpha-\alpha_0)t$ as in equations (40), equation (C2) becomes

$$h(t)=\frac{\mathrm{e}^{-\alpha_0 t}}{t^{\lambda+1}}\int_0^{t\Delta\alpha}u^\lambda F(\alpha_0+u/t)\,\mathrm{e}^{-u}\,\mathrm{d}u. \tag{C3}$$

At long times we obtain in place of equations (42) and (43):

$$\lim_{t\to\infty}[h(t)t^{\lambda+1}\,\mathrm{e}^{\alpha_0 t}]=F(\alpha_0)\int_0^\infty u^\lambda\,\mathrm{e}^{-u}\,\mathrm{d}u=F(\alpha_0)\Gamma(\lambda+1), \tag{C4}$$

$$h(t)\approx\Gamma(\lambda+1)F(\alpha_0)\,\mathrm{e}^{-\alpha_0 t}/t^{\lambda+1} \tag{C5}$$

where $\Gamma(\lambda+1)$ is the gamma function. An alternative derivation of these results is given by Doetsch (1974). With $\lambda=0$ we recover equations (42) and (43).

For the purpose of extrapolating data from some time t_0 onwards, equation (C5) contains three adjustable parameters. If we write

$$\lambda+1=-C, \qquad \alpha_0=-B, \qquad F(\alpha_0)=\mathrm{e}^A/\Gamma(\lambda+1), \tag{C6}$$

the parameters could be obtained from a least squares fit of the model

$$\ln h(t)=A+Bt+C\ln t \tag{C7}$$

to sufficiently numerous and accurate venous data. We hope to discuss elsewhere these computational problems in relation to real data.

A more detailed specification of $G(\alpha)$ would determine a time-course of the approach to the asymptotic form. For example, if in equation (C1) we choose $F(\alpha)=0$ for $\alpha<\alpha_0$, and

$$F(\alpha)=F(\alpha_0)\,\mathrm{e}^{-(\alpha-\alpha_0)/\beta}, \qquad \alpha\geq\alpha_0, \tag{C8}$$

with positive constants β and $F(\alpha_0)$, then $G(\alpha)$ has the form of a Pearson Type III distribution (Abramowitz & Stegun, 1965). Substituting from equation (C8) in equation (C2) with $\Delta\alpha = \infty$, and transforming the resulting integral to a gamma function, we obtain

$$h(t) = \Gamma(\lambda + 1) F(\alpha_0)\, e^{-\alpha_0 t}/(\beta^{-1} + t)^{\lambda+1}. \tag{C9}$$

The additional parameter β^{-1} determines the time-scale on which equation (C9) approaches equation (C5). Equation (C9) was derived in a statistical context by Turner (1963) for the case $\alpha_0 = 0$.

For $\lambda = 0$ the Pearson Type III distribution is reduced to the corresponding exponential distribution, and equation (C9) describes a time-course of the approach to the two-parametric asymptotic form given by equation (43). A different time-course of approach to that asymptotic form has already been exemplified in equation (44), based on a rectangular distribution of $G(\alpha)$. In equation (44) the time-scale of the approach was determined by $(\Delta\alpha)^{-1}$ rather than by β^{-1}.